

**GENERATION OF 3-D PROFILES OF THIN
FOLDED STRUCTURES USING PHASE SHIFT
FRINGE PROJECTION**

SUGANANDHA BHARATHI

UNIVERSITI SAINS MALAYSIA

2008

**GENERATION OF 3-D PROFILES OF THIN FOLDED STRUCTURES USING
PHASE SHIFT FRINGE PROJECTION**

by

SUGANANDHA BHARATHI

**Thesis submitted in fulfillment of the requirements
for the degree of
Master of Science**

~~September~~ February 2007 2008

ACKNOWLEDGEMENTS

First of all, I would like to take this opportunity to thank my supervisor Associate Professor Dr.Mani Maran Ratnam for his support, motivation and inspirational supervising through out the research and thesis writing process. In many stages of the research, his profound expertise and professional knowledge provided key injection to the technical solutions. Without his effort and guidance, this research would never have been completed. I also wish to express my sincere thank to Mechanical Engineering Workshop staff for their co-operation during the fabrication for the experimental setup.

I would like to thank my parents, wife and daughter for their support, patient and understanding, without which I could not have been able to complete my Master degree programme.

Last but not least, my sincere thanks to the School of Mechanical Engineering, University Science of Malaysia and the Ministry of Science, Technology and Environment (Malaysia) for the offer of the IRPA that enabled this work to be carried out.

TABLE OF CONTENTS

| | Page |
|---|--------------------------------------|
| ACKNOWLEDGEMENTS | ii |
| TABLE OF CONTENTS | iii |
| LIST OF TABLES | vi |
| LIST OF FIGURES | vii |
| LIST OF SYMBOLS | xiii xiv |
| LIST OF ABBREVIATION | xvi |
| ABSTRAK | xvii |
| ABSTRACT | xviii xix |
| CHAPTER ONE : INTRODUCTION | |
| 1.1 Background of research | 1 |
| 1.2 Problem statement | 4 |
| 1.3 Research objectives | 5 |
| 1.4 Research approach | 6 |
| 1.5 Thesis outline | 8 |
| CHAPTER TWO : LITERATURE REVIEW | |
| 2.1 Introduction | 10 |
| 2.2 General optical measuring method and their applications | 10 |
| 2.3 Fringe projection | 13 14 |
| 2.4 Calibration | 15 16 |
| 2.5 Digital processing technique | 20 22 |
| 2.6 Summary | 24 26 |

CHAPTER THREE : EXPERIMENTAL SETUP, DETERMINATION OF SCALING FACTOR AND PROJECTION ANGLE

| | | |
|-----|---|----------------------|
| 3.1 | Introduction | 2628 |
| 3.2 | Experimental setup | 2628 |
| 3.3 | Image distortion verification and determination of average scaling factor | 3436 |
| | 3.3.1 Results and discussion | 4244 |
| 3.4 | Determination of projection angle | 4547 |
| | 3.4.1 Theory | 4547 |
| | 3.4.2 Procedure | 4951 |
| | 3.4.3 Results and discussion | 6668 |
| 3.5 | Summary | 7072 |

CHAPTER FOUR : DEVELOPMENT OF AN ALGORITHM FOR GENERATING 3-D SURFACE USING PHASE SHIFTING WITH PHASE UNWRAPPING METHOD AND VERIFICATION ON ACTUAL ZIG – ZAG PATTERN

| | | |
|-----|---|------------------------|
| 4.1 | Introduction | 7473 |
| 4.2 | Development of algorithm and application on simulation images | 7274 |
| | 4.2.1 Development of three phase shifted simulated images | 7375 |
| | 4.2.2 Theory on phase shifting with phase unwrapping method | 8483 |
| | 4.2.3 Result and discussion | 8991 |
| 4.3 | Verification of phase shifting with phase unwrapping method on actual zig–zag pattern | 96105 |
| | 4.3.1 Experimental setup | 97106 |
| | 4.3.2 Procedure | 104108 |
| | 4.3.3 Result and discussion | 113120 |

| | | |
|-----|---------|------------------------|
| 4.4 | Summary | 422129 |
|-----|---------|------------------------|

CHAPTER FIVE : [MEASUREMENT GENERATION](#) OF 3-D SURFACE OF A LIVE FOLDED LEAF USING PHASE-SHIFTING METHOD

| | | |
|-----|--|------------------------|
| 5.1 | Introduction | 425132 |
| 5.2 | Approach 1Original method | 425132 |
| 5.3 | Approach 2Changes – Step one | 425132 |
| 5.4 | Approach 3Changes – Step two | 431138 |
| 5.5 | Result and discussion | 432139 |
| 5.6 | Summary | 437145 |

CHAPTER SIX : CONCLUSIONS AND FUTURE RESEARCH

| | | |
|-----|------------------------------------|------------------------|
| 6.1 | Conclusion | 438146 |
| 6.2 | Contributions of the research | 440148 |
| 6.3 | Recommendation for future research | 441149 |

| | |
|------------|------------------------|
| REFERENCES | 444152 |
|------------|------------------------|

| | |
|---------------------------------|------------------------|
| LIST OF PUBLICATIONS & SEMINARS | 447155 |
|---------------------------------|------------------------|

LIST OF TABLES

| | Page |
|--|------|
| Table 3.1 Distance between vertical lines and scaling factor determination | 44 |
| Table 3.2 Distance between horizontal lines and scaling factor determination | 45 |
| Table 3.3 Error in distance measured between vertical lines | 46 |
| Table 3.4 Error in distance measured between horizontal lines | 46 |
| Table 3.5 Tabulation of projection angles at various predefined i coordinate | 69 |
| Table 3.6 Tabulation of theoretical projection angle along i coordinate | 70 |
| Table 4.1 Tabulation of phase adjustment required | 87 |
| Table 4.2 Conditions for phase adjustment | 87 |
| Table 4.3 Mean and standard deviation of error along profile A (j=10 pixels) | 120 |
| Table 4.4 Mean and standard deviation of error along profile B (j=121 pixels) | 121 |
| Table 4.5 Mean and standard deviation of error along profile C (j=232 pixels) | 121 |
| Table 4.6 Mean and standard deviation of error along profile D (j=343 pixels) | 122 |
| Table 4.7 Mean and standard deviation of error along profile E (j=444 pixels) | 122 |
| Table 4.8 Increase in error for using a particular combination of filtering process along all the profiles | 123 |

LIST OF FIGURES

| | Page |
|-------------|------|
| Figure 1.1 | 1 |
| Figure 1.2 | 6 |
| Figure 3.1 | 28 |
| Figure 3.2 | 29 |
| Figure 3.3 | 29 |
| Figure 3.4 | 30 |
| Figure 3.5 | 31 |
| Figure 3.6 | 31 |
| Figure 3.7 | 32 |
| Figure 3.8 | 32 |
| Figure 3.9 | 33 |
| Figure 3.10 | 33 |
| Figure 3.11 | 34 |
| Figure 3.12 | 35 |
| Figure 3.13 | 36 |
| Figure 3.14 | 37 |
| Figure 3.15 | 37 |
| Figure 3.16 | 38 |
| Figure 3.17 | 39 |
| Figure 3.18 | 40 |
| Figure 3.19 | 40 |

| | | |
|-------------|---|----|
| Figure 3.20 | Intensity profile of grid lines image | 41 |
| Figure 3.21 | Measurement points for determining radial distortion and scaling factor | 42 |
| Figure 3.22 | Measuring points for verifying the average scaling factor | 43 |
| Figure 3.23 | View of line projected on flat surface | 47 |
| Figure 3.24 | View of line projected on object placed on flat surface | 48 |
| Figure 3.25 | The projection and viewing directions and the fringe break | 49 |
| Figure 3.26 | Types of ray | 50 |
| Figure 3.27 | Image of shifted fringe pattern | 52 |
| Figure 3.28 | Flow chart of the program for obtaining projection angle | 53 |
| Figure 3.29 | Image loaded | 54 |
| Figure 3.30 | Arrays of pixels | 54 |
| Figure 3.31 | Original image coordinate and required field of view region | 55 |
| Figure 3.32 | Cropped image | 55 |
| Figure 3.33 | Region to be applied median filtering | 56 |
| Figure 3.34 | Filtering mask | 56 |
| Figure 3.35 | Filtering process | 56 |
| Figure 3.36 | Indicating cell position | 57 |
| Figure 3.37 | Array containing gray level of pixels after median filtering | 57 |
| Figure 3.38 | Average filtering mask | 58 |
| Figure 3.39 | Indicating cell position | 58 |
| Figure 3.40 | Array containing gray level of pixels after average filtering | 59 |
| Figure 3.41 | Average filtered image coordinate and required field of view region | 59 |
| Figure 3.42 | Array containing gray level of pixels before and after cropping process | 60 |
| Figure 3.43 | Cropped image after filtering process | 60 |
| Figure 3.44 | Threshold image | 61 |
| Figure 3.45 | Image after thinning process | 61 |

| | | |
|-------------|--|----|
| Figure 3.46 | Portion of image on Figure 3.45 | 62 |
| Figure 3.47 | Image as Figure 3.46 | 62 |
| Figure 3.48 | Simplification of experimental setup, 1 st step | 64 |
| Figure 3.49 | Simplification of experimental setup, 2 nd step | 65 |
| Figure 3.50 | Simplification of experimental setup, 3 rd step | 65 |
| Figure 3.51 | 3-D view of Figure 3.50 | 66 |
| Figure 4.1 | Flow chart of the program for extracting the 3-D surface data from simulation images | 74 |
| Figure 4.2 | Cosine function | 75 |
| Figure 4.3 | Cosine function against j coordinate | 76 |
| Figure 4.4 | Cosine function with amplitude between 127.5 to -127.5 | 77 |
| Figure 4.5 | Intensity against j coordinate | 78 |
| Figure 4.6 | 0, $2\pi/3$, $4\pi/3$ phase shifted sinusoidal wave | 79 |
| Figure 4.7 | Viewing position shift due to height | 80 |
| Figure 4.8 | Cross section along any j coordinate for rectangle object placed on the background | 81 |
| Figure 4.9 | Cross section along any j coordinate for zig-zag pattern placed on the background | 81 |
| Figure 4.10 | Triangle of same sides | 82 |
| Figure 4.11 | Distance traveled horizontally and height same | 82 |
| Figure 4.12 | Movement of viewing position due to height | 84 |
| Figure 4.13 | Array containing wrapped phase data | 89 |
| Figure 4.14 | 0 phase shifted without object | 91 |
| Figure 4.15 | $2\pi/3$ phase shifted without object | 91 |
| Figure 4.16 | $4\pi/3$ phase shifted without object | 91 |
| Figure 4.17 | 0 phase shifted with rectangle object | 92 |
| Figure 4.18 | $2\pi/3$ phase shifted with rectangle object | 92 |
| Figure 4.19 | $4\pi/3$ phase shifted with rectangle object | 92 |
| Figure 4.20 | 0 phase shifted with zig-zag pattern | 93 |

| | | |
|-------------|--|-----|
| Figure 4.21 | $2\pi/3$ phase shifted with zig-zag pattern | 93 |
| Figure 4.22 | $4\pi/3$ phase shifted with zig-zag pattern | 93 |
| Figure 4.23 | Phase map image for rectangle pattern | 94 |
| Figure 4.24 | Phase map image for zig-zag pattern | 94 |
| Figure 4.25 | 3-D height profile for rectangle pattern placed on background | 95 |
| Figure 4.26 | 3-D height profile for zig-zag pattern placed on background | 95 |
| Figure 4.27 | Section view along $j=10$ for rectangle | 96 |
| Figure 4.28 | Section view along $j=125$ for rectangle | 96 |
| Figure 4.29 | Section view along $j=240$ for rectangle | 97 |
| Figure 4.30 | Section view along $j=10$ for zig-zag pattern | 97 |
| Figure 4.31 | Section view along $j=125$ for zig-zag pattern | 97 |
| Figure 4.32 | Section view along $j=240$ for zig-zag pattern | 98 |
| Figure 4.33 | 0 phase shifted with rectangle object for projection angle of 50.7° | 99 |
| Figure 4.34 | $2\pi/3$ phase shifted with rectangle object for projection angle 50.7° | 99 |
| Figure 4.35 | $4\pi/3$ phase shifted with rectangle object for projection angle 50.7° | 99 |
| Figure 4.36 | 0 phase shifted with zig-zag pattern for projection angle 50.7° | 100 |
| Figure 4.37 | $2\pi/3$ phase shifted with zig-zag pattern for projection angle 50.7° | 100 |
| Figure 4.38 | $4\pi/3$ phase shifted with zig-zag pattern for projection angle 50.7° | 100 |
| Figure 4.39 | Phase map image for rectangle pattern with projection angle 50.7° | 101 |
| Figure 4.40 | Phase map image for zig-zag pattern with projection angle 50.7° | 101 |
| Figure 4.41 | 3-D height profile for rectangle pattern placed on background with projection angle 50.7° | 102 |
| Figure 4.42 | 3-D height profile for zig-zag pattern placed on background with projection angle 50.7° | 102 |

| | | |
|-------------|---|-----|
| Figure 4.43 | Section view along $j=10$ for rectangle with projection angle 50.7° | 103 |
| Figure 4.44 | Section view along $j=125$ for rectangle with projection angle 50.7° | 103 |
| Figure 4.45 | Section view along $j=240$ for rectangle with projection angle 50.7° | 104 |
| Figure 4.46 | Section view along $j=10$ for zig-zag pattern with projection angle 50.7° | 104 |
| Figure 4.47 | Section view along $j=125$ for zig-zag pattern with projection angle 50.7° | 104 |
| Figure 4.48 | Section view along $j=240$ for zig-zag pattern with projection angle 50.7° | 105 |
| Figure 4.49 | Glass plate placed on the support frame | 106 |
| Figure 4.50 | Angle bars placed onto the painted glass plate | 106 |
| Figure 4.51 | Portion of the side view of Figure 4.50 | 107 |
| Figure 4.52 | Cross sectional dimension of the angle bar | 107 |
| Figure 4.53 | Profile view of the angle bar placed onto glass plate generated using phase shifting method | 108 |
| Figure 4.54 | Flow chart for extracting the 3-D surface data from actual images | 109 |
| Figure 4.55 | 0 Phase shift image with angle bars | 110 |
| Figure 4.56 | $2\pi/3$ Phase shift image with angle bars | 110 |
| Figure 4.57 | $4\pi/3$ Phase shift image with angle bars | 110 |
| Figure 4.58 | 0 Phase shift image without angle bars | 111 |
| Figure 4.59 | $2\pi/3$ Phase shift image without angle bars | 111 |
| Figure 4.60 | $4\pi/3$ Phase shift image without angle bars | 111 |
| Figure 4.61 | Original image coordinate and required field of view region | 112 |
| Figure 4.62 | 1 st Crop of 0 phase shift image with angle bars | 113 |
| Figure 4.63 | 1 st Crop of $2\pi/3$ phase shift image with angle bars | 113 |
| Figure 4.64 | 1 st Crop of $4\pi/3$ phase shift image with angle bars | 113 |
| Figure 4.65 | 1 st Crop of 0 phase shift image without angle bars | 114 |

| | | |
|-------------|--|-----|
| Figure 4.66 | 1 st Crop of $2\pi/3$ phase shift image without angle bars | 114 |
| Figure 4.67 | 1 st Crop of $4\pi/3$ phase shift image without angle bars | 114 |
| Figure 4.68 | Image size after 1 st cropping and required field of view | 115 |
| Figure 4.69 | Phase map image with angle bars | 116 |
| Figure 4.70 | Phase map image without angle bars | 116 |
| Figure 4.71 | 3-D surface plot of the zig –zag pattern produced using angle bars | 117 |
| Figure 4.72 | Height profiles (0,232) to (435,232) | 118 |
| Figure 4.73 | Height profiles (0,232) to (435,232) after height adjustment | 119 |
| Figure 4.74 | Region around the edges of the angle bars | 124 |
| Figure 4.75 | 3-D surface plot of the zig–zag pattern after height adjustment | 125 |
| Figure 4.76 | Comparison between actual and reference heights along Profile A (along $j=7.34$ mm) | 126 |
| Figure 4.77 | Comparison between actual and reference heights along Profile B (along $j=88.8$ mm) | 126 |
| Figure 4.78 | Comparison between actual and reference heights along Profile C (along $j=170.3$ mm) | 127 |
| Figure 4.79 | Comparison between actual and reference heights along Profile D (along $j=251.8$ mm) | 127 |
| Figure 4.80 | Comparison between actual and reference heights along Profile E (along $j=325.9$ mm) | 128 |
| Figure 5.1 | Array containing wrapped phase data with focus on region I | 133 |
| Figure 5.2 | Array containing wrapped phase data with focus on region II | 135 |
| Figure 5.3 | Array containing wrapped phase data with focus on region III | 136 |
| Figure 5.4 | Array containing wrapped phase data with focus on region IV | 137 |
| Figure 5.5 | Leaf reference image | 138 |
| Figure 5.6 | 0 phase shift image of the leaf | 139 |
| Figure 5.7 | $2\pi/3$ phase shift image of the leaf | 139 |
| Figure 5.8 | $4\pi/3$ phase shift image of the leaf | 140 |

| | | |
|-------------|--|-----|
| Figure 5.9 | Cropped 0 phase shift image of the leaf | 140 |
| Figure 5.10 | Cropped $2\pi/3$ phase shift image of the leaf | 141 |
| Figure 5.11 | Cropped $4\pi/3$ phase shift image of the leaf | 141 |
| Figure 5.12 | Phase map image of the leaf | 142 |
| Figure 5.13 | 3-D surface of the leaf using original method | 143 |
| Figure 5.14 | 3-D surface of the leaf after step one changes | 143 |
| Figure 5.15 | 3-D surface of the leaf after step two changes | 144 |

LIST OF SYMBOLS

| | |
|---------------------------|---|
| D | Actual distance between two adjacent dark fringes |
| i | Horizontal coordinate |
| j | Vertical coordinate |
| Δy | Amount of shift by fringe (mm) |
| h | Height |
| θ | Projection angle |
| Δy_{image} | Amount of shift by fringe (pixels) |
| f | scaling factor |
| j_1 | Vertical coordinate at point 1 |
| j_2 | Vertical coordinate at point 2 |
| j_{base} | Vertical coordinate on reference line |
| j_{shift} | Vertical coordinate on the shifted line |
| θ_{rad} | Angle in radian |
| $F(j)$ | One dimensional cosine function |
| $F(i,j)$ | Two dimensional cosine function |
| S_H | Horizontal distance |
| S_V | Vertical distance |
| ΔS_H | Difference in horizontal distance |
| ΔS_V | Difference in vertical distance |
| Δi | Difference in i coordinate |
| x | Distance between adjacent maximum intensity of projected fringe |
| y | Distance between adjacent maximum intensity of reflected fringe |
| θ_i | Angle of incidence or projection angle |

| | |
|-----------------------|--|
| $I_b(i,j)$ | Gray scale intensity on the background |
| $I_o(i,j)$ | Gray scale intensity on the object |
| $A(i,j)$ | Uniform background intensity |
| $B(i,j)$ | Amplitude of sinusoidally varying component of intensity |
| $\phi(i,j)$ | Phase angle |
| $\Delta\phi(i,j)$ | Phase shift |
| ϕ_t | Wrapped phase |
| $P_{\text{map}}(i,j)$ | Phase map |
| H_{Adj} | Adjusted height |
| H_{Obj} | Height with object |
| H_{Wobj} | Height without object |

LIST OF ABBREVIATION

| | |
|------|---|
| CAD | Computer aided design |
| CCD | Charged coupled device |
| CMM | Coordinate measuring machine |
| ESPI | Electronic speckle pattern interferometry |
| DLP | Digital light processing |
| DMD | Digital micromirror device |
| LCD | Liquid crystal display |
| PC | Personal computer |
| LUT | Look-up table |
| FFT | Fast fourier transform |
| MIL | Matrox Imaging Library |
| FOV | Field of view |
| TIFF | Tagged image file format |

PENGUKURAN GENERASI PENJANAAN PROFIL--PROFIL PERMUKAAN

TIGA-DIMENSI BAGI DAUN JOHANNESTEIJSMANIA

ALTIFRONS STRUKTUR-STRUKTUR BERLIPAT NIPIS DENGAN

MENGGUNAKAN KAEDAH UNJURAN PINGGIR ANJAKAN FASA

ABSTRAK

Struktur plat berlipat yang ber dinding nipis biasanya digunakan dalam reka bentuk struktur kerana ia mempunyai kombinasi unik iaitu struktur, fungsi salutan, kecekapan berat dan bentuk yang menarik dari segi estetik. Reka bentuk struktur plat berlipat berdasarkan struktur berlipat semulajadi seperti daun *johannesteijsmania altifrons* belum lagi diterokai. Faedah utama daun berlipat berkenaan ialah ia disokong oleh hanya satu batang utama. Faedah ini dapat dieksploitasi dalam reka bentuk struktur jika permukaan 3-D daun berkenaan diketahui. Oleh sebab daun ini mudah cangga atau rosak jika pengukuran dilakukan dengan menggunakan kaedah konvensional, kaedah pengukuran tanpa penyentuhan dibangunkan untuk mengukur tinggi pada semua titik di atas permukaan tiga-dimensi permukaan daun. Dengan menggunakan data tinggi berikut, permukaan tiga-dimensi (3-D) daun dapat dibina dengan menggunakan perisian CAD untuk tujuan analisis. Tiga corak pinggir telah diunjurkan pada permukaan dengan menggunakan projector-projector slaid. Setiap corak pinggir yang diunjur mempunyai anjakan fasa 0, $2\pi/3$, $4\pi/3$. Imej ketiga-tiga anjakan fasa unjuran pinggir yang telah dicangga oleh permukaan objek telah dirakam dengan menggunakan sebuah kamera CCD. Data 3-D permukaan objek didapati dengan menggunakan algoritma 'phase unwrapping'. Algoritma telah disahkan dengan menggunakan imej anjakan fasa simulasi sebelum menggunakannya ke atas imej anjakan fasa yang sebenar. Peralatan eksperimen yang mudah telah diwujudkan untuk merakam imej tiga anjakan fasa pinggir yang telah diunjurkan ke atas objek.

Pengesahan telah dikendalikan untuk memastikan sama ada terdapat sebarang erotan kanta pada kamera CCD. Didapati bahawa tiada sebarang erotan kanta pada kamera CCD. Faktor skala purata 0.734 mm/pixels dan sudut unjuran 50.7° telah didapati secara eksperimen dan disahkan. Ralat maxima kerana penggunaan faktor skala purata adalah 1.2%. Pengesahan kaedah anjakan fasa telah dilakukan menggunakan objek sebenar di mana palang bersudut digunakan untuk membentuk corak bengkok-bengkok. Ralat maxima purata 7.2% telah diperolehi. Walaupun terdapat ralat pada medan pemandangan disebabkan oleh beberapa ~~factor~~faktor, data permukaan 3-D dapat dibina. Dengan menggunakan kaedah anjakan fasa, data permukaan 3-D daun telah dibina.

GENERATION OF 3-D PROFILES OF THIN FOLDED STRUCTURES USING PHASE SHIFT FRINGE PROJECTION

ABSTRACT

Thin walled folded plate structures are commonly used in structural designs due to their unique combination of structural and cladding functions, weight efficiency and aesthetically appealing form. However, the design of folded plate structures based on naturally occurring folded structures such as the *johannesteijsmania altifrons* leaf is relatively unexplored. The main advantage of this particular type of folded leaf is that it is supported by a single main stem. This advantage can be exploited in structural designs if the 3-D surface form is known. Since the leaf can easily deform or be damaged if measured using conventional contact methods, the non-contact phase-shifting fringe projection method was developed for extracting the 3-D surface data of the leaf. Using the surface data the 3-D surface of the leaf could be constructed with the CAD software for analysis. Three fringe patterns were projected onto the surface using a slide projector each with phase-shift of 0, $2\pi/3$ and $4\pi/3$. The three phase-shifted fringe patterns deformed by the object surface were captured using a CCD camera. The 3-D data of the object surface were reconstructed using a phase unwrapping algorithm. The algorithm was verified using simulated phase shifted images before applying to actual phase shifted image. A simple experimental apparatus were setup for capturing the actual three phase shifted fringe which are projected onto the object. Verification was done for confirmation whether there is any lens distortion on the CCD camera. It was found that there was no lens distortion on the CCD camera. The average scaling factor of 0.734 mm/pixels and the projection angle of 50.7° were obtained experimental and were verified. The maximum error due to usage of average scale factor was found to be 1.2%. Verification of the phase

shifting method were done using actual object where angle bars are used to form zig – zag pattern. Average maximum percentage error of 7.2% was obtained. Although there is error along the field of view due to various factors, the 3-D surface data construction was possible. Using the phase shifting method the 3-D surface data of the leaf was obtained.

CHAPTER 1

INTRODUCTION

1.1 Background of research

Thin walled folded plate structures are widely used in various modern industrial areas due to their unique advantages such as combining of structural and cladding functions, weight efficiency and aesthetically pleasing structural form. Due to the numerous advantages of the folded plate structures, extensive work has been carried out and reported in the finite element modeling (FEM) of such structures for construction applications (Gotsulyak *et al.*, 2000, Samanta [_and Mukhopadhyay *et al.*](#), 1999, Yuanming *et al.*, 2000, Ahmed *et al.*, 2000, Lee *et al.*, 1995).

However, modeling of folded plate structures based on naturally occurring folded structures such as the *johannesteijsmania altifrons* leaf as shown in Figure 1.1 has not been explored and the advantages of the natural structure has not been exploited in real design application.



Figure 1.1: The *johannesteijsmania altifrons* plant

The unique advantage of modeling the structure based on the *johannesteijsmania altifrons* leaf is that the leaf is supported by a single main stem and this advantage can be exploited in the structural design.

There are various measurement techniques available for the 3-D measurement of surface forms. They can be generalised into contact and non-contact measuring technique. In the case of contact techniques the surface 3-D coordinates are obtained by the touch of the probe onto the surface. One of the widely used contact measurements is Coordinate Measuring Machine (CMM). A CMM requires point-by-point scanning which is time consuming. Also the contacting nature of CMM does not allow measurement of delicate surfaces (Huang [et al-P.S-et al.](#), 2003). Since, a leaf is of low stiffness and fragile, it deforms when touched. Therefore, the contact method could not be used to measure the 3-D surface of the leaf being studied in this research.

In the case of non-contact method, the laser scanning method is commonly used to extract 3-D information. In this method line-by-line scanning is carried out. The problem with this method is that scanning is a time consuming process and since the leaf is alive, it will vibrate as well as move due to floor vibration or even slight wind blowing which could not be controlled with current experimental setup. Therefore, due to these uncontrollable factors, error in measurement during the line scanning will be unavoidable.

Optical measurement methods are becoming popular due to their speed, accuracy, sensitivity as well as non-destructive characteristics (Huang [et al-P.S-et al.](#), 2003). Three dimensional object shape and its surface roughness have been widely investigated using optical measurement techniques based on structured lighting (Richard [Kowarschik-et al.](#), 2000). Structured lighting method is also known as fringe projection. In this method, the fringe pattern that is varying sinusoidally is projected

onto the object of interest and at the point of variation in height the fringe pattern will be shifted. From this amount of shift the height of the object at that point is calculated. This process is repeated for every point on the surface and the 3-D surface of the object could be obtained.

The structured light that is projected could be either collimated light or non-collimated light. The advantage of the collimated light is that the light rays will be parallel to each other and therefore the projection angle of the light onto the object of interest will be constant. The disadvantage is that due to projector lens size constraint, the region that the collimated light covers is small and therefore if a large object is used then the object needs to be divided into smaller regions. Then the collimated light is projected onto each of the regions and then the 3-D data obtained need to be patched up so that the 3-D surface of the object can be generated. This is a very slow and complicated process. Collimated light projecting equipment is also expensive.

The advantage of using non-collimated light is that the area the projection covered is large. The disadvantage of using non-collimated projection is that the projection angle at every point on the object surface will vary. This method will avoid the need for patching up all the 3-D data to form the surface of the object as non-collimated light covers a larger region. Non-collimated light projecting equipment is less expensive. Due to these advantages, non-collimated light is used in this research.

Phase-shifting method is widely used compared to single fringe projection method. This is because phase-shifting method can reduce error obtained using single fringe projection method (Mani Maran Ratnam *et al.*, 1999). Another advantage of phase-shifting method over single fringe projection method is that the 3-D data at every point can be obtained instead along fringes only. In phase shifting method, three images of object projected with the fringe pattern of phase shifting zero, $2\pi/3$ and $4\pi/3$

are recorded. Using these three images, the wrapped phase is then calculated. Using phase unwrapping method the wrapped phase are unwrapped and from the unwrapped phase the 3-D surface of the object can be calculated.

1.2 Problem Statement

~~Before the finite element analysis could be applied onto a structure resembling the 3-D surface of the *johannesteijsmania altifrons* leaf, the 3-D surface data of the leaf surface need to be acquired. There are various ways in obtaining the 3-D measurement of the leaf, that is contact and non-contact method. The commonly used method would be contact method like Coordinate Measurement Method. It is found that the leaf easily deforms upon even light contact. Therefore, contact method would not be suitable for obtaining the 3-D measurement of the leaf. The cross sectional view of the leaf could not be obtained by cutting the leaf because leaf loses its form, that is the zig-zag pattern slopes becomes less steep once the leaf is cut along the cross section.~~

~~In case of the non-contact method using fringe projection, the variation in intensity of the fringe projected onto the object of interest captured by the CCD camera will be used to find the amount of shift in the fringe due to the variation in the height of the object surface. Based on the amount of shift of the fringe pattern the height at a particular point is calculated.~~

~~An automatic technique for extracting the 3-D surface data of the leaf using phase shifting with phase unwrapping method will be developed in this research.~~

Phase shifting with phase unwrapping method had not been used to reconstruct the 3-D surface of naturally occurring folded structures such as *johannesteijsmania altifrons* leaf. The 3-D surface data of the leaf is not available for reconstruction of the leaf. There are various ways in obtaining the 3-D surface data of the leaf that is contact

and non-contact method. The commonly used method would be contact method like Coordinate Measurement Method. Since the leaf deforms easily upon even light contact, contact method would not be suitable for obtaining the 3-D surface data of the leaf. The leaf also loses its zig-zag appearance when it is cut to obtain its cross section dimension. Therefore the 3-D surface data of the leaf could not be verified using existing measuring techniques. The proposed method has to be verified before can be used to extract the 3-D surface data of the leaf.

An automatic technique for extracting the 3-D surface data of the leaf using phase shifting with phase unwrapping method will be developed in this research. The proposed method will be verified using zig-zag pattern where the dimensions are known before using the method to extract the 3-D surface data of the leaf.

1.3 Research objectives

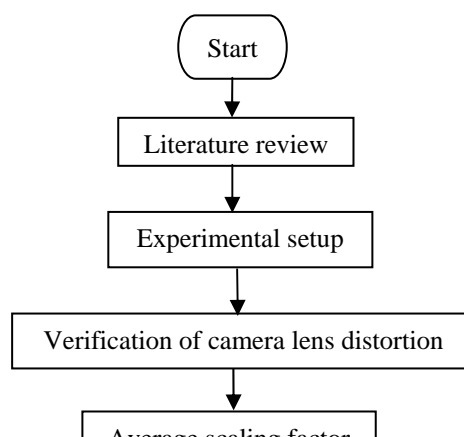
The main objective of this research is to develop a non-contacting optical technique to measure the 3-D surface of the living folded leaf using phase shifting with phase unwrapping method.

To achieve the main objective, three sub-objectives of the research have been identified, including:

- (a) To obtain the average scaling factor that can be used to convert the dimension in the image to the actual physical dimension.
- (b) To obtain the projection angle that will be used during calculation of the height at various points.
- (c) To develop a program that uses phase-shifting with phase unwrapping method on the actual phase shifted images of the leaf to obtain the 3-D surface of the leaf.

1.4 Research approach

Figure 1.2 shows the flow chart on the research approach adopted in this research work.



First of all, literature on development of 3-D surface of living folded leaf using phase shifting with phase unwrapping method will be reviewed. Past research will be reviewed thoroughly to determine the current state of [the](#) art in this research.

Based on orientation and size of the leaf, the experimental setup will be developed with the equipment available for this research. There are various types of camera lens distortion that could be present with the CCD camera. Therefore

verification will be done to see if there is any camera lens distortion. Then the average scaling factor will be calculated. It is the factor that is required to be multiplied with the distance in the image captured by the CCD camera to obtain the actual distance.

Fringe pattern are projection from a slide projector onto 12 glass stripes placed with intervals of 10 mm between each other. The dimension of each glass stripe is 10 mm of width, 3 mm of height and 400 mm of length. The resultant image of the fringe pattern is captured using a CCD camera placed perpendicular to the surface of the glass stripe. From the captured image of the glass stripes covered with fringe pattern, the projection angle is calculated. Comparison will be done between the projected angle obtained experimentally and projection angle obtained theoretically.

A program will be developed to simulate phase shifted image due to placing of a rectangle or zig-zag pattern on the background. Then the program will use this simulated images to develop the 3-D surface of the rectangle as well as the zig-zag pattern using phase shifting with phase unwrapping method. The actual phase shifted images of the angle bars arranged in zig-zag pattern are captured using the experimental setup. Then the program used on the simulation image is modified such that it will load these phase-shifted images and develop the 3-D surface of the actual zig-zag pattern. Along few profiles, the error between actual and the one obtained using the program are calculated.

Finally using the experimental setup the actual phase shifted images of the leaf are captured. The program used for developing 3-D surface of actual zig-zag are modified such that it will load the phase shifted images of the leaf and from this image the 3-D surface of the leaf is obtained.

1.5 Thesis outline

This thesis is arranged in accordance to the objectives and approach mentioned above. Chapter 2 presents the basic concept of phase shifting process and also the various non-contact methods used in obtaining the 3-D surface of object. Reviews on the related research from the early stage until recent years on the development of 3-D surface using phase shifting method are presented.

Chapter 3 discusses in details the experimental setup. Using the experimental setup the average scaling factor and projection angle are calculated.

Chapter 4 deals with simulation of phase shifted images if a rectangle object placed on a background and also if a zig-zag pattern placed on a background. Using phase shifting with phase unwrapping method the 3-D surface of the rectangle and zig-zag pattern are obtained. Using the experimental setup, actual phase shifted images of angle bars placed such that it forms zig-zag pattern are obtained. The phase-shifted images are captured using CCD camera and transferred into the computer with the help of a frame grabber. Using phase shifting with phase unwrapping method the 3-D surface of the actual zig-zag pattern are obtained. The 3-D surface obtained is verified with the reference data.

Chapter 5 deals with capturing of phase-shifted image of the actual folded leaf using the experimental setup. Then using the phase shifting with phase unwrapping method, the 3-D surface of the leaf are developed. The field number formula is slightly modified in order for obtaining the 3-D surface of the leaf.

Finally, conclusions of this research are drawn in Chapter 6. Recommendations and suggestions for future research are also provided.

CHAPTER 2

LITERATURE REVIEW

2.1 Introduction

In this chapter, a few types of optical measuring techniques that are widely used will be discussed briefly. Literature study will be conducted in order to obtain more information on the following :-

- Optical measuring technique to be used.
- Experimental setup.
- Digital processing technique to be used.
- Object worked on by previous researches.

It is very important to obtain more information on the above points as it will indicate the advantages and limitations of the past researches in order to determine the proper technique and procedure to be adopted in this research for obtaining the 3-D surface of the folded leaf.

The main reason for exploring into the type of object that the previous researchers had worked on is to see what difficulty that they had encountered and whether any of them had worked on the folded leaf structure.

2.2 General optical measuring method and their applications

Contact types of measuring techniques are widely used, for example the coordinate measuring machine (CMM). CMM requires point-by-point scanning, which is time consuming and also contact nature does not allow measurement of delicate surfaces (Huang *et al*, 2003). Optical methods are becoming popular due to its speed, accuracy, sensitivity, non-contact and non-destructive.

Wolfgang Osten (2000) had used holographic interferometry to obtain high precision displacement data in the range of the wavelength of the laser light. Holographic interferometry was used to obtain the relationship between phase difference or phase shift and displacement. Problem related to optical measuring are phase measurement, calibration, data processing and data presentation. The experimental setup as well as the procedures is found to be complicated

Jeong and Kim (2002) had used high speed moiré method of color gratings projection, which performs phase-shifting 3-D contouring with only a single operation of fringe capturing. Three red, green and blue pairs of projection and viewing gratings were fabricated on a single glass plate with predetermined lateral offsets. The glass plate is translated along with the color gratings during measurement at a fast speed, so that a color CCD camera simultaneously monitors three separate patterns of moiré fringes with $2\pi/3$ phase offset. In case of moiré method two grating are required that are reference grating and projection grating and this gratings must undergo translation motion. Therefore the experimental setup for moiré method is expensive and complicated. It is also found that it is important to adjust the mean intensities and visibilities of each RGB moiré fringes to be of same level in order to avoid any error in measurement. This method also found to be sensitive to the colour of the target as the captured moiré fringes are affected by the varying reflectance of the target surface which could result in error in measurement.

Xie and Atkinson (1997) had discussed about usage of absolute moiré contouring technique for measuring 3-D object. The grating which was a sinusoidal wave intensity grating was mounted on a bearing rotated by a stepper motor. The object was located behind this grating. The grating was illuminated by a light source which are having the same vertical height from grating as the CCD camera. The

shadow of the grating falls onto the object. This moiré contour pattern was focused by lens and a CCD camera took the image. Using this method, three dimensional surfaces of concave and convex objects were reconstructed. The major drawback of this method is that if the grating is not perfect, the measuring accuracy will be affected.

Ritter *et al* (1997) discussed the application of ESPI for 3-D deformation measurement in material testing and dimensioning of structures and quality control that require a stable and compact interferometric device. This device was realized by optoelectronic components as laser diodes, fiber optics and CCD cameras. The developed interferometer is not only suitable for analysis of static problems, but also for measurements of vibration behavior of objects in real-time, by intensity modulation of the illuminating laser light. Disturbing influences of oscillating rigid body movements between ESPI and the considered object can be eliminated by a Michelson interferometer, which is adapted to the ESPI. By applying phase shifting techniques to the recorded speckle patterns, results of high accuracy can be achieved. The experimental setup is complicated and expensive.

Harizanova and Sainov (2006) proposed double symmetrical illumination and double symmetrical observation experimental approaches for 3-D surface measurement using fringe projection method. The influence of shadowing and respectively information losses due to complicated relief are overcome using this method. The advantage of the method is that the 3-D measurement of an object can be carried out without usage of reference plane. The experimental setup is expensive and complicated.

Mani Maran Ratnam (2000) had used phase shifting method to detect the edge of object of interest, which is placed in a homogenous background. The author found that when using phase shifting method the error is less compared to the other edge

detection method. The author also stated that the accuracy is unaffected by background noise and the accuracy is much more higher compared to analysis carried out using the original fringe pattern images. Mani Maran Ratnam (2003) had also used phase shift fringe projection method to measure the 3-D shape of multi surface object in a homogeneous background that is 2-rectangle box of different sizes arranged in stack.

Several techniques are available for measuring surface profiles. These include moiré contouring, ESPI method, holographic contouring and fringe projection. Fringe projection has several advantages over the others because:-

- (a) Experimental design and analysis technique is simple.
- (b) No costly optical components or instruments are required.
- (c) Information can be extracted from a single fringe pattern.
- (d) Good contrast fringes could be obtained.

By using phase shifting method, the error in measurement obtained when using single fringe projected image can be reduced.

Dhanasekar and Ramamoorthy (2008) stated that measurement of diffuse surface is easy using moiré and fringe projection method. Compared to fringe projection method, moiré method is sometimes tedious and time consuming to evaluate quantitative data from fringe pattern. Fringe projection method was used to assess the machined surface roughness.

Chen *et al* (2005) had stated that moiré method application for large object measurement is limited by the size of the gratings and the measurement accuracy is dependent on the resolution of the gratings. The advantage of interferometry techniques is that high accuracy can be achieved but the surface of test object must be

highly reflective and monochromatic light must be used. The reasoning was more favoring fringe projection method.

It was found that various types of method are used for obtaining the 3-D data using optical method. It was found that Fourier Transform although uses a single image to obtain the 3-D data, is very complicated process. Phase shifting was used by most of the researchers as it is very easy and the accuracy is much more higher compared to analysis carried out using the original single fringe projected onto object image.

2.3 Fringe projection

Mani Maran Ratnam (2000) had used slide projector to project the fringe pattern onto the object and the object covered with fringe pattern is captured using digital camera. The phase shifting was done using a rotary mirror. This is a non-collimated method and the experimental setup is simple and also less expensive.

Mani Maran Ratnam *et al* (1999) generated the fringe pattern using laser beam. Beam from 7mW He-Ne laser was split into two using beam splitter and this two rays will be reflected from the two mirrors will undergo interference to form fringe pattern. The experimental setup is complex as the beam needs to be split properly in order for interference which results in fringe pattern can be obtained.

Huang *et al* (2003) had used digital light processing (DLP) projector, which is using digital micromirror device (DMD) technology. The fringe pattern are created using software and the fringe pattern is projected onto the object of study using the DLP. Therefore, phase shifting can be done on the PC and projected directly from PC onto the object using the DLP. These will result in accurate phase shifting and also phase shifting can be done quickly. 3-D surface of object of plaster head and human face was developed.

Huang *et al* (1999) had used digital fringe projection for detecting and measuring the corrosion of engineering structures. The fringe pattern was generated and also phase shifting was done by using software. By generating the fringe pattern by software, the intensity, phase and fringe spacing can be changed instantly. Digital Light Processing (DLP) was used to project the fringe pattern onto the object. This fringe pattern will be of high brightness and contrast ratio. LCD panels lack of image quality, brightness and contrast ratio.

Quan *et al* (1999) had launched the light from a laser into a single mode optical fiber. This is then coupled into two optical fibers using a 50/50 fused coupler. The outputs of the two fibers are used as two point sources. The sources are coherent source. The sinusoidal linear fringes are produced by the interference of the two point sources. Since the distance from the point sources to the screen is large compared to distance between the point sources, Young's fringe patterns will be formed on the observation screen. The fringe patterns are captured using a camera and camera negatives are used as the gratings for fringe projection.

Zhang *et al* (2000) and Lilley *et al* (2000) had used twin fiber interferometer for producing fringe pattern. The fringe spacing and orientation can be varied by moving the ends of the fibers relative to each other.

Bulut and Inci (2005) had developed three dimensional optical profilometry using four – core optical fiber. Fourier transform method was used to extract the 3-D data from the fringe pattern. The experimental setup and the procedure are complex. More over, phase shifting method accuracy is much better than Fourier transform method.

Various techniques for producing fringe patterns and also phase shifting of the fringe pattern adopted by researchers. It was found that usage of slide projector seems to be simpler. The fringe patterns will be captured on the slide and phase shifting will be done using the rotary mirror. DLP will be a better solution as it simplifies the experimental setup and error due to manual phase shifting will be eliminated as phase shifting was done on PC directly and projected via DLP onto the object from PC. Since DLP apparatus is expensive and was not available for the research work, slide projector will be used for projecting the fringe pattern onto the object and rotary mirror will be used for phase shifting the fringe pattern manually.

2.4 Calibration

Calibration of the experimental apparatus is very important in order to obtain the multiplying factor known as scaling factor, which will be multiplied with the image distance in terms of the number of pixels to obtain the actual distance in millimeter. It is also essential to identify if there are any lens distortion that need to be rectified by using transformation matrix before finding the actual distance from the image distance.

Mani Maran Ratnam *et al* (1999) had verified the error due to aberrations in the camera's optical system using a high quality graph paper 80 mm x 80 mm which was photographed and digitized into grid points. Using the digitised points the scaling factor were calculated and using this scaling factor, the distance in the image and the corresponding actual distance were compared.

Tian *et al* (2008) had discussed about calibration where calibration target of known dimension image were captured and the error between the measured and actual dimension were verified. After the verification, the system is calibrated and using the calibrated system, the 3-D surface of statue was reconstructed. The statue's dimension is unknown. Verification of the measurement of the statue was not carried

out as the system had been verified using object of known dimension. These approach will be adopted in the current research where using object of known dimension the proposed method are verified before using the method to reconstruct 3-D surface of object with its dimension not known.

Tkaczyk and Jóźwicki (2002) studied the influence of an imaging system on the measurement error in coherent fringe projection method. They found that wave aberrations of imaging system has significant influence on the measurement error. The measurement error increases as the changes in height increases. The influence of aberrations is difficult to reduce by calibration due to their different influence for different object height gradients. It was found that incoherent methods are less sensitive to environmental disturbances and can be used for larger fields.

Sitnik *et al* (2002) had combined fringe – gray code projection technique for obtaining the 360-degree shape measurement. To avoid the influence of unknown aberration characteristics introduced by the projector and camera objectives on accuracy, pre calibration of the measurement volume is applied. The calibration and measurement processes are verified by analysis of sample objects where separate cloud of points is automatically merged into main cloud. Calibration at various planes is obtained. Identical markers (circle of a particular radius) of equal interval forming array with center circle larger and used for obtaining the calibration matrix for various z distance. 360-degree surface of Elenie's Bust statue was developed.

Spagnolo *et al* (2000) had shown how height calibration was done. Mathematical solution on obtaining the height based on the projection angle of non-collimated projection and the viewing angle of the camera which varies theoretically. A point on the object will be at different point on the reference plane which is placed in

between the object and the camera as the viewing direction are converging to the lens of camera.

Reich *et al* (2000) proposed a new concept for 3-D shape measurement of complex objects based on photogrammetry and fringe projection. Usually in fringe projection technique, one projector is used for projecting the fringe pattern and one camera is used for capturing the object covered with fringe pattern. Here two cameras were used. Calibration using photogrammetry technique was carried out in order to obtain the relative coordinate of the two cameras as well as the transformation of views of the cameras into global coordinate. This way the cameras orientation with respect to their relative position is fixed and can be moved to obtain the 3-D shape of complex shape. Calibration of the two cameras as well as the transformation of views to global coordinates uses very complicated process.

Lilley *et al* (2000) used empirical calibration method that does not rely on direct measurement of these geometrical parameters of the optical system or mathematical model as it is found that small error in fringe spacing, magnification factors and angle θ between viewing and illumination optics produce large error in final calculated height value.

Calibration was done in 3 steps:-

1. A disc of known diameter placed on a reference plane and the image is captured. From the image the scaling factor is calculated.
2. Then 3-D shape of a flat plane is measured and by subtracting this reconstructed surface from all subsequently measured object, the effect of misalignment of the projection system and distortions of imaging system are reduced.

3. A wedge having crosses at regular interval and the crosses height exactly known image are captured. The relation between the height and the corresponding measured phase using the least square fit a line of height versus phase and from that a direct phase to height multiplier value obtained.

Schreiber and Notni (2000) had used self- calibrating fringe projection systems created based on the concepts of photogrammetry. Surplus measurement values required for self-calibration method. A special fringe projection technique with a rotating grating and multiple cameras and projection positions was used. The authors stated the advantages of their approach that are:-

- (1) Self-calibration is possible without the use of calibration equipment.
- (2) Full body measurement can be realized without the use of matching procedures or target points.
- (3) Since phase values used to calculate the coordinates and system parameters like image quality of the cameras has no influence on measurement accuracy.

Liu *et al* (2003) proposed an accurate calibration based on phase-shifting measurement technique for measuring the absolute 3-D surface profiles. The system distortions for each detection location were calibrated individually. These mean that each pixel is calibrated individually. Varying the position of flat surface and measuring the corresponding phase obtained, the phase to height relationship was obtained. It is found that the method proposed involves complicated mathematical approach and also the object used is not complex type but smooth variation of height type, therefore noise will be less.

Liang and Su (1997) discussed computer simulation of three-dimensional sensing with structured illumination. Phase shifting method was used. The development of deformed fringe pattern due to the 3-D surface and construction of the 3-D surface from the deformed fringe pattern are explained. The main parameters that determine the measurement were the distance of the camera from the reference plane, the fringe pitch and also the distance between camera and projector. These parameters need to be adjusted until the error obtained in obtaining the 3-D surface of any object is minimised.

Echigo (1989) mentioned that there are various factors determine the transformation from 2-D camera image to the 3-D coordinate. It is split into two, one is the intrinsic parameter and the second one is extrinsic parameter. Intrinsic parameters are like distance of the lens from the image plane and also the image plane center from the lens center. Extrinsic parameters are like the translational position of camera with respect to global coordinate system and also rotational position of camera with respect to the method that are adopted, the image center and the translation and rotational position can be determined independency. In this way the error can be isolated and not propagated. The calibration was done using a set of parallel lines.

Shih *et al* (1995) had investigated the effect of neglecting lens distortion in camera calibration. Errors could be caused by observation error of 2-D image points, the radial lens distortion coefficient, image size and resolution. Guidelines for engineers to use on deciding when to consider lens distortion in camera calibration was provided. Focus was more on the radial distortion.

Park and Hong (2001) proposed two methods for calculating camera lens distortion for real-time applications. Lens distortion problem can be ignored for constant parameter lenses that is focal length field. In case of zoom lenses, the focal length

changes, so lens distortion is essential before camera calibration. The two methods proposed are look-up table (LUT) of focal length and lens distortion which can be constructed in the initialisation process. The second one is a feature-based method that is all collinear points, in real object must be also collinear in the image, the radial distortion coefficient are varied until the error in collinearity is minimised. This method calculates lens distortion using nonlinear optimization. Once the lens distortion has been calculated, the camera calibration will be done.

Salvi *et al* (2002) did a detailed review of some of the most used calibration techniques, in which the principal idea has been to present them all with the same notation. Comparison was done using same real points. It is found that non-linear technique accuracy was much better than the linear method. Modeling of radial distortion is quite sufficient when high accuracy is required. The use of complicated models does not improve the accuracy significantly.

Zhang *et al* (2004) had analysed the measurement performance of a 3-D full field imaging system based on the projection of grating and active triangulation. Mathematical relationship between height, phase and the structural parameters were explored. The height details were obtained based on mathematical relationship without considering optical distortion or electronic noise. In the actual image there will be optical distortion and electronic noise, which must be taken into account for determination of height from phase details.

Researchers in the past have stressed on camera calibration as it provides the relationship between the distance measured on the captured image with the actual distance. Unlike previous work, a simple method will be adopted in this research for finding the relation between the distance measured on the captured image with the actual distance, which is known as scaling factor. Using grid lines, which are captured

using the CCD camera, the scaling factor will be calculated. Radial distortion is a major concern among the researchers. Therefore, confirmation will be done to see if there is any radial distortion due to the CCD camera used in the research work.

2.5 Digital processing technique

Huang *et al* (2003) had used colour in retrieving the 3-D information of the object surface. It was found that measurement errors could be introduced by the original colour of the object surface if it were not neutral. In order to avoid this kind of problem, gray scale value image will be used in the current research work.

Hobson *et al* (1997) had used digital signal processing in order to conduct the phase demodulation and phase unwrapping to obtain the 3-D surface. Digital filters were used to remove component of the intensity so that the phase shift can be obtained from it. The author states that phase deviation is not a true demodulator as it gives the total signal phase rather than the required phase deviation. The author mentioned that intensity is modified by noise, by variation in surface colour and texture and possible due to non – uniform lighting. The author found that there is increase in noise as step or discontinuity is approached. The formula proposed by the author will be used in current work to obtain the height using phase shifting method.

Large areas are subdivided to partially overlapping regions and the 3-D data of these sub regions are obtained and this overlapping sub regions are patched to obtain single 3-D surfaces (Wolfgang Osten, 2000). Absolute phase values were obtained from the captured images and from that the 3-D surface is found. 3-D surface of the car brake saddle was developed.

Chen *et al* (2005) had used sawtooth type fringe pattern rather than sinusoidal type fringe pattern due to similar characteristic between sawtooth and wrapped phase.

By means of linear translation, wrapped phase data are extracted from recorded intensity pattern. Using phase unwrapping the phase is unwrapped and height were obtained. Comparison where done with results obtained using phase shifting method and found that phase shifting method accuracy is better than proposed method.

He *et al* (1998) had used Fast Fourier Transform (FFT) and signal-demodulating techniques to determine the height from the object covered with fringe pattern image. Fringe pattern are projected onto reference and object and the resultant images are captured. Both the intensity images are applied Fourier Transform and then the Fourier Spectra component is isolated from the other components of the Fourier Transform. Inverse Fourier is applied on this Fourier spectra and the phase angle at various point are obtained from arc tan of imaginary part divide by real part of the result obtained from the inverse Fourier Transform. The difference in the phase angle between reference phase angle and object phase angle at a particular point will give the phase shift which will be used for calculating the height at that point.

Charette and Hunter (1996) presented phase unwrapping on noisy phase. The method first identifies distinct regions between boundaries in an image and then phase shifting the regions with respect to one other and adding 2π to unwrap the phase. Image pixels are segmented between interfringe and fringe boundary by fitting a plane model using least squares to overlapping domains centered on all pixels.

Li and Su (2002) had carried out phase unwrapping based on combination of modulation and phase fitting reliability. Modulation means that if there is phase jump which is more than $\pm\pi$ then the phase at that point need to be added or subtracted 2π to make the phase continuous. There will always be faulty phase jump due to complex reflectivity and quasisanded object, noises such as saturation/cut-off and quasispeckle in the fringe image. This faulty phase pixels are known as unreliable phase. All

unreliable phase pixels will be identified and the rest known as reliable phase pixels. This method is known as phase fitting reliability. Phase unwrapping will be done in sequence for all the reliable phase pixels, before applying on the unreliable phase pixels. In this way, error will be isolated and not propagated throughout the field. 3-D surface of a model head was developed. The process for identifying unreliable phase pixels is complex and complicated.

Spagnolo *et al* (2000) used fringe projection method with Fourier Transform method to obtain the 3-D surface. The sensitivity of the method, defined as the amount of phase change for a given height, increases with angle of projection with the normal to the incidence plane and inversely proportional to the fringe spacing. 3-D object of ancient Sestertius of the Emperor Galba, ancient etruscan votive lamp and statue of the Apostle St. Matthew were developed.

Fringe projection of different orientation and wavelength are projected onto the object and from this the beat frequency is obtained. Using the phase of this beat frequency, the phase is unwrapped and from the unwrapped phase the height is obtained. Cameras with their relative distance fixed are placed at different location to capture difference regions of the object. From this difference regions (partial views) 3-D coordinate are obtained using photogrammetry technique (Reich *et al.*, 2000). 3-D surface of car door was developed.

Hung *et al* (2000) had used phase stepping method with 4 frames to obtain the 3-D surface of the object. Calibration technique is introduced to relate the grating phase and the surface depth/slope thus eliminating the use of complicated mathematical relationship. Initially the phase distribution for planar surface is obtained. Then the phase distribution of unknown surface is obtained. The two-phase distribution will be subtracted. These difference divide by the optical setup constant will provide the